

Spin dynamics in CuO and $\text{Cu}_{1-x}\text{Li}_x\text{O}$ from ^{63}Cu and ^7Li nuclear relaxation

P. Carretta, M. Corti, and A. Rigamonti

Department of Physics "Alessandro Volta," University of Pavia, Via Bassi 6, 27100 Pavia, Italy

(Received 22 September 1992)

^{63}Cu nuclear quadrupole resonance (NQR), nuclear antiferromagnetic resonance (AFNMR), and spin-lattice relaxation, as well as ^7Li NMR and relaxation measurements in CuO and in $\text{Cu}_{1-x}\text{Li}_x\text{O}$, are used to study the spin dynamics in the paramagnetic and in the antiferromagnetic (AF) phase, and in particular the effects induced by lithium doping. It is argued that Li enters in CuO lattice up to a doping x around 4%; from a comparison of the electric-field gradient (EFG) and of the dipolar field at the nucleus with theoretical estimates, it appears that Li^+ is slightly displaced from the Cu lattice site. From NQR, NMR, and AFNMR spectra, information on the Cu hyperfine interaction and the EFG are derived. The Néel temperature T_N is affected by Li doping to a moderate extent, decreasing from 226 K in CuO to $T_N = 183$ K for $x = 3.7\%$. The relaxation rates, driven by the time-dependent part of the magnetic electron-nucleus Hamiltonians, indicate that the Cu^{2+} spin dynamics is almost unaffected by Li doping for $T \gg T_N$ and possibly controlled by valence fluctuations. The Li doping modifies in a dramatic way the spin fluctuations in the AF phase. The relaxation rates in $\text{Cu}_{1-x}\text{Li}_x\text{O}$, in fact, increase by orders of magnitude (similarly to the case of copper-oxide precursors of high- T_c superconductors) and display temperature behaviors quite different from those in CuO. These effects are associated with an effective low-frequency spectral density of the spin fluctuations negligible in CuO, which strongly increases upon Li doping. This increase is related to the fluctuations induced in the local Cu^{2+} spin configuration as a consequence of the diffusionlike motion of the holes in the AF matrix, implying the resurgence of low-frequency spin excitations. The orders of magnitude of the relaxation rates, their dependences on x and on T , as well as on the measuring frequency, are satisfactorily explained by a picture in which the correlation time τ_h for the hole-hopping motion is controlled by an energy gap $E(x)$ between localized and itinerant states. Quantitative information on τ_h and $E(x)$ is thus derived.

I. INTRODUCTION

One of the most debated issues in the field of high- T_c superconductivity is the role of the Cu^{2+} correlated spin dynamics in the CuO_2 planes of the oxide superconductors. This fact has stimulated several recent studies of the static and dynamic magnetic properties of bulk CuO.¹ This compound crystallizes in a monoclinic phase, with the Cu atom coordinated with four coplanar oxygens forming an almost rectangular parallelogram. The oxygen is coordinated with four Cu's to form a distorted tetrahedron.² The lattice constants are $a = 4.68$ Å, $b = 3.42$ Å, and $c = 5.13$ Å, with the angle $\beta = 99.54^\circ$. In terms of magnetic properties, the CuO structure can be viewed as consisting of chains along the [101] direction, with a Cu-O-Cu angle of 145° , giving rise to a quasi-one-dimensional (1D) superexchange coupling. The Cu-O-Cu bond angle in the other directions, in fact, is near to 90° and this should lead to smaller exchange interactions.

CuO presents many magnetic and electronic properties similar to those of undoped copper oxides, such as La_2CuO_4 . It is considered a Mott-Hubbard insulator with a gap of the charge-transfer type, and the antiferromagnetic (AF) long-range order sets in below a transition temperature T_N around 230 K. From T_N down to about 212 K the magnetic phase is incommensurate, while below this temperature a commensurate phase is formed with characteristic wave vector $\mathbf{q}_{\text{AF}} = 0.5\mathbf{a}^*, 0, -0.5\mathbf{c}^*$.^{1,3,4} The uniform magnetic susceptibility displays a broad maximum around 540 K, a feature typical of low dimensional systems.⁵⁻⁸ Magneti-

zation⁹ and specific-heat measurements^{10,5} also indicate low dimensional correlations of the AF interactions.

A very interesting aspect of CuO is the possibility of doping with Li, without affecting the oxygen stoichiometry. Magnetic-susceptibility measurements in a sample with 1% of Li have been reported.¹¹ The precise localization of Li^+ is under debate. In this paper it will be shown that Li^+ can actually be incorporated in the unit cell up to an extent of doping around 4%, and indirect evidence will be given that Li^+ substitutes a Cu^{2+} ion, taking a position slightly displaced from the Cu lattice site. The charge unbalancement due to the heterovalent substitution is expected to induce extra holes in the Cu-O band, a feature equivalent to the Ba or Sr substitution for La in La_2CuO_4 . As will be discussed later on, the transition temperature is slightly affected by Li doping and the Cu^{2+} spin dynamics in the paramagnetic (P) phase appears to retain most of the essential aspects occurring in pure CuO. On the contrary, in the AF phase a relevant effect of the charge defect on the Cu^{2+} spin excitations is observed.

^{63}Cu nuclear quadrupole resonance (NQR) measurements in pure CuO have been reported, providing the estimate of the electric-field gradient (EFG) and information on the spin dynamics in the P phase.^{12,13} ^{63}Cu nuclear resonance in the AF phase yielded the evaluation of the hyperfine field and of the EFG tensor at the Cu nucleus, at 4.2 K.¹⁴ The complete assignment of the Cu EFG tensor has been obtained in the P phase from NMR-NQR experiments on a single crystal.¹⁵

This paper reports a thorough NQR-NMR study of

CuO and $\text{Cu}_{1-x}\text{Li}_x\text{O}$ carried out in the temperature range 3.5–370 K by means of ^{63}Cu and ^7Li resonances. The main purpose has been to achieve insights on the correlated spin dynamics and on the effects related to the charge doping of the AF matrix, particularly in the light of the correspondent situation occurring in high- T_c superconductors. The paper is organized as follows: Sec. II deals with the experimental aspects and presents the experimental results of static character, such as ^{63}Cu NQR quadrupole coupling constant, ^7Li NMR spectra in the P phase as well as ^{63}Cu AFNMR and ^7Li NMR in the AF phases. Then the data pertaining to the Cu^{2+} spin dynamics, namely ^{63}Cu NQR and ^7Li NMR relaxation rates in both P and AF phases are presented. Section III is devoted to the analysis of the experimental results in terms of the EFG's, magnetic fields, transition temperatures, and their x dependences. Emphasis is given to the interpretation of the relaxation rates in terms of spin excitations and to the effects of Li^+ doping on the Cu^{2+} correlated spin dynamics. Summarizing remarks and conclusions are presented in Sec. IV.

II. EXPERIMENTALS AND EXPERIMENTAL RESULTS

A. Samples

CuO was prepared by sintering in oxygen flow for 24 h at 950°C 5N powder. The samples were then cooled at room temperature in oxygen atmosphere through successive temperature steps, in about 10 h. Thermogravimetric analysis showed a stoichiometric ratio of Cu:O equal to one, within the sensitivity of the technique. Oxygen deficient samples CuO, with $x \geq 0.95$ were also prepared, by heating in high vacuum. Li-doped samples were prepared in the same way by adding 5N pure Li_2O in the proper stoichiometry to the CuO powder.¹⁶

From Li NMR spectra and from the recovery laws of the relaxation process (see details later on) the Li content could be determined. It turned out that phase segregation occurred from Li percent $x \geq 4\%$. Samples with nominally higher Li content appeared to have no more than that amount incorporated in the CuO matrix.

B. NQR and NMR general aspects

The ^{63}Cu NQR and the ^7Li NMR measurements have been carried out by means of a Bruker MSL200 spectrometer with a high-power unit allowing a radio frequency (rf) field H_1 of amplitude around 100 G. The temperature range of the measurements was 3.5–370 K, with thermal stability within a tenth of a degree. ^7Li NMR spectra have been obtained by Fourier transforming half of the echo signal following the quadrupolar echo pulse sequence $(\pi/2)_x - \tau - (a\pi/2)_y, \pi/2$ corresponding to the pulse length maximizing the signal in a solution of LiCl. In view of the small quadrupole coupling constant the spread of the ^7Li NMR frequency due to the angular dependent quadrupole perturbation is smaller than the radio frequency spectral distribution. Thus, in practice, both the central ($\frac{1}{2} \rightarrow -\frac{1}{2}$) and the two satellites ($\pm\frac{3}{2} \rightarrow \pm\frac{1}{2}$) lines are irradiated. The signal, in fact, was maximized by a pulse length equal to the one in the LiCl

solution, where the static quadrupole interaction is averaged to zero. For $a=2$ the quadrupolar echo sequence is expected to generate an echo from the central line (which is broadened by second-order quadrupole effects and other magnetic mechanisms). For $a=1$ the satellites transitions, broadened by first-order quadrupole interaction, are also refocused in the echo. The spectrum, in fact, showed a strong central line, broadened mainly by magnetic interactions and two less intense shoulders of the satellite lines spread by the quadrupolar interaction. Below T_N the ^7Li NMR line shows a further broadening due to the dipolar field from Cu^{2+} spins.

^{63}Cu resonance was detected in the pure NQR regime in the P phase and in the quadrupole perturbed NMR regime in the internal AF field (AFNMR) below T_N . The ^{63}Cu NQR spectra have been obtained through the amplitude of the quadrupolar echo on sweeping the irradiation frequency, with H_1 at moderate level. Even in pure CuO no free-induction decay was observable, consistently with a width of the NQR line around 80 KHz, a feature common to most NQR lines in the magnetic cuprates and possibly related to a distribution of EFG's due to strains and defects. Upon Li doping the copper NQR line shows a further marked broadening, with a linewidth [full width half intensity (FWHI)] around 1 MHz. The typical Cu NQR spectrum for Li content of 3% is shown in Fig. 1(a).

In the AF phase the hyperfine field at the Cu nucleus is 11.7 T, as derived by Tsuda *et al.*¹⁴ Figure 1(b) shows the ^{63}Cu quadrupole perturbed AFNMR spectrum ob-

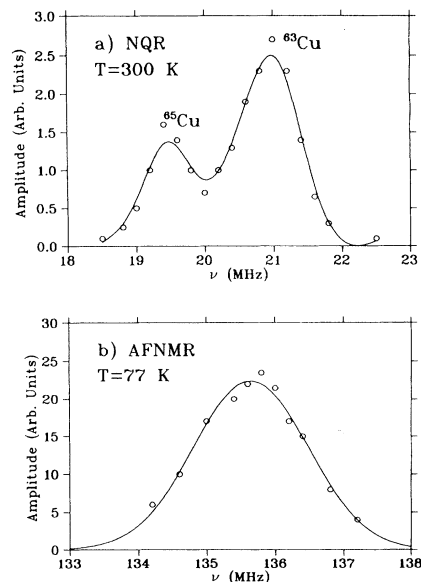


FIG. 1. (a) Copper NQR spectrum, obtained from the amplitude of the quadrupolar echo on sweeping the irradiation frequency, in $\text{Cu}_{0.97}\text{Li}_{0.03}\text{O}$, at $T=300$ K (the lines are guides to the eye). The spectrum is remarkably broader ($\delta_{\text{FWHI}}^{63} \approx 1$ MHz) than the one in pure CuO ($\delta_{\text{FWHI}}^{63} \approx 80$ KHz). (b) ^{63}Cu AFNMR spectrum of the central ($\frac{1}{2} \rightarrow -\frac{1}{2}$) line in the AF phase of $\text{Cu}_{0.97}\text{Li}_{0.03}\text{O}$, at $T=77$ K. In pure CuO this resonance occurs practically at the same frequency, with linewidth $\delta_{\text{FWHI}}^{63} \approx 300$ KHz.

tained in Cu_{0.97}Li_{0.03}O for the ($\frac{1}{2} \rightarrow -\frac{1}{2}$) transition. Some extra broadening of the line occurs also in this case (in pure CuO the FWHI is around 300 KHz).

The nuclear-spin-lattice relaxation measurements have been carried out from the recovery of the echo signal after a sequence of saturating pulses at the central frequency of the correspondent spectrum. For the ⁶³Cu NQR relaxation the saturation was obtained with a few rf pulses, separated by a time much longer than the spin-spin dephasing time T_2 . No contribution from fast spin-diffusion process was observed in the recovery at short times, indicating saturation of the full line. The recovery is well described by a single exponential law, yielding $T_1^{-1} = 6W$, W being the relaxation rate associated with the time dependence of the magnetic Hamiltonian. A relaxation process driven by the magnetic mechanism was supported by the comparison of the relaxation rates for the ⁶⁵Cu and ⁶³Cu isotopes, which scale with the square of the correspondent gyromagnetic ratios. A possible distinct behavior in the NQR response for those Cu nuclei having an immediate Li neighbor in the doped samples was not resolved as separate line. On the other hand, the occurrence of a common spin temperature is expected to induce a recovery process described by a single exponential.

Below T_N , in the AFNMR regime, the ⁶³Cu Zeeman levels are perturbed by the static quadrupole interaction and the recovery of the central line is no longer described by an exponential law. From the solution of the master equations one obtains for the recovery law

$$\frac{s(\infty) - s(t)}{s(\infty)} = ce^{-12Wt} + (1-c)e^{-2Wt}, \quad (1)$$

with the constant c depending on the duration Δ of the saturation sequence. For $\Delta \ll W^{-1}$ (fast saturation of the central line only) $c=0.9$. For $\Delta \gg W^{-1}$ the equilibrium initial populations of the levels lead to $c=0.6$. Both the experimental conditions of fast and long saturation were often used, yielding consistent results and a more precise evaluation of W . For pure CuO at low temperatures, due to the extremely long T_1 , only the condition of fast saturation was used.

In the ⁷Li NMR relaxation measurements, all the lines are practically irradiated and the recovery is well described by a single exponential law, with no dependence on the length of the saturating sequence. The time constant of the recovery is $T_1 = (2W)^{-1}$.

C. Spectra and fields

The temperature dependence of the ⁶³Cu NQR frequency in the P phase, for pure CuO and for Li-doped CuO, is shown in Fig. 2. For pure CuO, from the center of the ⁶³Cu line the resonance frequency ν_R can be estimated with an error of about ± 10 KHz. For $I = \frac{3}{2}$ one has

$$\nu_R = \nu_{\pm 3/2 \rightarrow \pm 1/2} = \nu_Q (1 + \eta^2/3)^{1/2}, \quad (2)$$

η being the asymmetry parameter. From the analysis of the quadrupole perturbed NMR spectra at 295 K one has $\eta = 0.26$.¹⁵ The extra broadening of the ⁶³Cu NQR lines

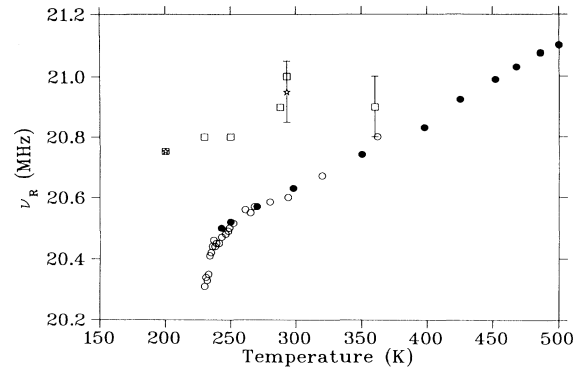


FIG. 2. ⁶³Cu NQR frequency in pure CuO (open circles present work, closed circles data from Ref. 13) and in Li-doped CuO (only representative points, squares Li content 3%, stars 3.7%) in the paramagnetic phases. The large error for the Li-doped samples reflects the broadening of the line [see Fig. 1(a)].

in the doped samples [see Fig. 1(a)] causes a large error in the evaluation of ν_R . However, an increase of about 400 KHz can be detected. The ⁶³Cu NQR measurements could not be extended very close to T_N due to a remarkable decrease of T_2 , which becomes around $3 \mu\text{s}$ for $T \approx T_N + 1$ K.

The ⁶³Cu AFNMR frequencies were found consistent to the ones obtained by Tsuda *et al.*¹⁴ in pure CuO. The temperature behavior of these frequencies has been reported¹⁵ and it is consistent with the findings through neutron scattering and μ^+ spin resonance (μ^+ SR). The ⁶³Cu AFNMR frequencies do not exhibit remarkable modifications upon Li doping, indicating that the hyperfine field is practically unaffected.

The ⁷Li NMR spectra above T_N show a small, temperature-independent shift of about 20 ppm with respect to a solution of LiCl. The temperature independence of the shift suggests the absence of a transferred hyperfine interaction at the Li site, consistent with a negligible overlap of the Li electronic states with the Cu 3d and/or O 2p orbitals. It can be recalled that the dipolar field due to the Cu²⁺ ions yields zero shift in a powdered sample.

The shape of the ⁷Li NMR spectra is related to the angular distribution of the frame of reference of the principal axis of the EFG tensor at the Li site with respect to the magnetic field \mathbf{H}_c . By diagonalizing the Hamiltonian

$$\mathcal{H} = -\gamma_{\text{Li}} \hbar \mathbf{I} \cdot \mathbf{H}_0 + eQIV \quad (3)$$

for different orientations of \mathbf{H}_0 with respect to the EFG \mathcal{V} , the spectra can be computationally reproduced fairly well. The comparison with the simulated spectra (Fig. 3) indicates for the ⁷Li quadrupole coupling constant, a value close to 100 KHz, while $\eta \approx 0.98$.

Below T_N the Li NMR line shows a sizeable broadening (Fig. 4), again with no detectable shift and consistent with the dipolar origin of the field \mathbf{h}_{Li} at the Li nucleus. The line shape can be obtained by considering the powder distribution of \mathbf{h}_{Li} with respect to \mathbf{H}_0 and one finds a rectangular shape of width $2\gamma|h|$. The comparison of the simulated ⁷Li NMR spectrum with the experimental one at $T = 25$ K, yields for the dipolar field $|\mathbf{h}_{\text{Li}}| = 500 \pm 50$ G.

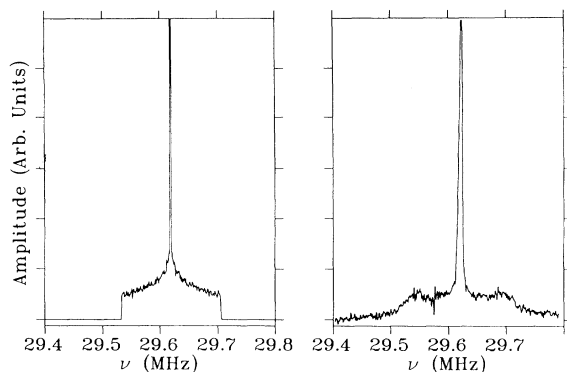


FIG. 3. Comparison of the simulated (left) ${}^7\text{Li}$ NMR quadrupole perturbed spectrum with the experimental one (right), in the paramagnetic phase ($T \approx 295$ K) of $\text{Cu}_{0.97}\text{Li}_{0.03}\text{O}$. The simulated spectrum corresponds to $H_0 = 1.8$ T and to an EFG tensor at Li nuclei characterized by $\eta = 0.98$ and $\nu_Q = 100$ KHz.

D. Relaxation rates

The ${}^{63}\text{Cu}$ NQR relaxation rates $6W$ in the P phases of $\text{Cu}_{1-x}\text{Li}_x\text{O}$ are reported in Fig. 5. The spin-spin relaxation time T_2 was occasionally measured and found shorter than T_1 by a factor of about 10, for $T \gg T_N$. The T_1/T_2 ratio increases by a factor of about 2 on approaching T_N . The Cu relaxation rates in the samples of CuO_x , with x up to 0.95, were found independent on the oxygen stoichiometry.

In Fig. 6 the ${}^7\text{Li}$ relaxation rates as a function of temperature, for two samples of $\text{Cu}_{1-x}\text{Li}_x\text{O}$ are shown. It should be remarked that the peak at high temperatures marks the Néel temperature (see later on), in agreement with the disappearing of the Cu NQR signal. No effect of the external magnetic field on T_N seems to be present, since specific-heat measurements show a peak at about the same temperatures. The Néel temperatures are reported in Table I. The marked peaks observed in $2W$ in the AF phases are related to the role of the charge defects as will be discussed in detail later on.

The ${}^{63}\text{Cu}$ AFNMR relaxation rates in the AF phases as a function of Li content, at $T = 77$ K and $T = 4.2$ K, are shown in Fig. 7. A remarkable finding is the marked increase of $2W$ with x .

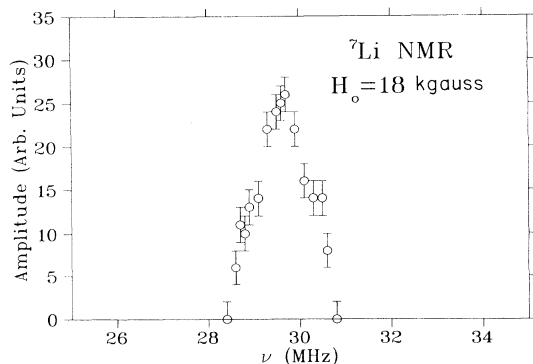


FIG. 4. ${}^7\text{Li}$ NMR spectrum in the AF phase of the 3% Li-doped CuO sample, at $T = 25$ K. The resonance line is broadened by the dipolar interaction, while no detectable shift is present.

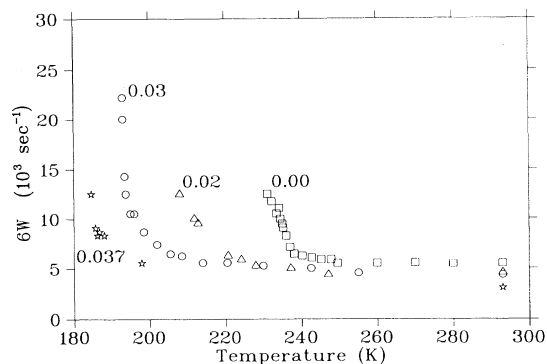


FIG. 5. ${}^{63}\text{Cu}$ NQR relaxation rates as a function of temperature in the paramagnetic phases of $\text{Cu}_{1-x}\text{Li}_x\text{O}$.

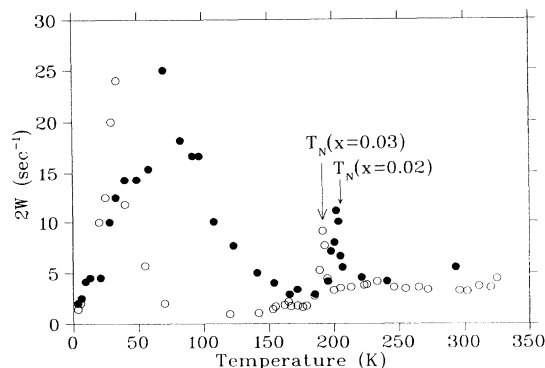


FIG. 6. ${}^7\text{Li}$ NMR spin lattice relaxation rate $2W$ in $\text{Cu}_{1-x}\text{Li}_x\text{O}$ as a function of temperature for $x = 0.03$ (open circles) and $x = 0.02$ (full circles).

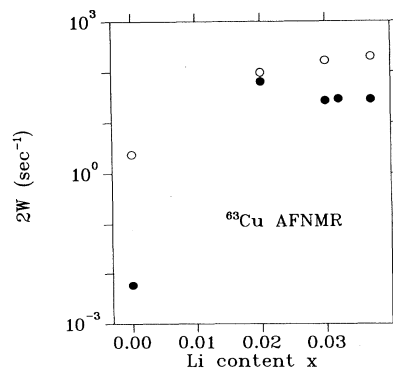


FIG. 7. ${}^{63}\text{Cu}$ AFNMR relaxation rates for the central ($\frac{1}{2} \rightarrow -\frac{1}{2}$) line in the AF phases of $\text{Cu}_{1-x}\text{Li}_x\text{O}$ as a function of Li content, at $T = 77$ K (open circles) and at $T = 4.2$ K (full circles).

TABLE I. Transition temperature from the *P* to the AF phase in Cu_{1-x}Li_xO, as a function of *x*, as obtained from a combination of ⁷Li NMR relaxation rate and specific-heat measurements.

<i>x</i>	<i>T_N</i> (K)
0.00	226±1
0.02	205±1
0.03	191.5±0.5
0.037	183±1

III. ANALYSIS OF THE DATA AND DISCUSSION

In this section the results pertaining to static quantities, such as EFG's and internal magnetic fields, and their dependence on temperature and Li content are discussed (Sec. III A). In Sec. III B the relaxation rates for Cu and Li, which are related to the time-dependent part of the magnetic nucleus-electron Hamiltonians, are analyzed in terms of spin dynamics and their *x* and *T* dependences in the AF phase will be discussed in some more detail.

A. Magnetic fields and EFG's

The temperature dependence of ⁶³Cu quadrupole coupling constant in the *P* phase (Fig. 2) shows two major features: ν_Q increases with temperature and has a rather marked minimum on approaching *T_N*.

The principal axes *z* of the EFG tensor is nearly normal to the plane of the four coplanar oxygens^{14,15} and \mathcal{V}_{zz} originates from two terms:

$$\mathcal{V}_{zz}^{\text{Cu}} = \mathcal{V}_{zz}^{\text{val}} + \mathcal{V}_{zz}^{\text{ion}} \quad (4)$$

the former being the term from 3*d* Cu valence electrons, while the latter is the contribution from the ionic charge distribution. It has been suggested^{17,18} that $\mathcal{V}_{zz}^{\text{ion}}$ is negative (corresponding to $\nu_Q^{\text{ion}} = -23.6$ MHz, for an antishielding factor $\gamma_\infty = -7.6$). Then $\mathcal{V}_{zz}^{\text{val}}$ is positive and it should correspond to a value for ν_Q^{val} around 44 MHz. Some covalency in the Cu-O bondings has also been inferred.^{15,18} The increase of ν_Q with temperature is likely to track a decrease of $\mathcal{V}_{zz}^{\text{ion}}$, a rather usual effect from lattice anharmonicity.

The broadening of the ⁶³Cu NQR line upon doping can result from the random effects on EFG's due to Li⁺ ions. The increase of ν_Q in Cu_{1-x}Li_xO with respect to CuO is likely to be related either to the charge unbalancement due to the extra holes which decreases $\mathcal{V}_{zz}^{\text{ion}}$ (similarly to what is observed in high-temperature superconductors¹⁹) or to the change in the occupation of the 3*d* orbitals through $\mathcal{V}_{zz}^{\text{val}}$ possibly as a result of internal pressure.¹⁸

The decrease of ν_Q for $T \rightarrow T_N^+$ is similar to the one expected when a structural transition is approached and the mean-square value of the fluctuating critical variable increases.²⁰ Thus it could indicate that the *P*-AF transition is accompanied by fluctuations of the electronic configuration. In fact, x-ray photoelectron spectroscopy shows that valence charge fluctuations, with strong electron-phonon coupling, occur in CuO.²¹ A more detailed analysis of this effect is prevented by the loss of the

NQR signal close to *T_N*.

As pointed out in Sec. II, an indirect estimate of the EFG at the Li site can be obtained from the quadrupole perturbed NMR spectrum. If Li occupies Cu site, the value of \mathcal{V}_{zz} for Li should correspond to $\mathcal{V}_{zz}^{\text{ion}}$ for Cu, after scaling with the ratio of the antishielding factors and of the quadrupole moments. Thus

$$(\nu_Q)_{\text{Li}} = (\nu_Q^{\text{ion}})_{\text{Cu}} \frac{(1 - \gamma_\infty^{\text{Li}})Q_{\text{Li}}}{(1 - \gamma_\infty^{\text{Cu}})Q_{\text{Cu}}} \approx 300 \text{ KHz}, \quad (5)$$

and $\eta \approx 0.26$, having used $\gamma_\infty^{\text{Cu}} = -7.6$, $\gamma_\infty^{\text{Li}} = 0.23$, $Q_{\text{Li}} = 0.03$ barn, $Q_{\text{Cu}} = 0.21$ barn, and $(\nu_Q^{\text{ion}})_{\text{Cu}} = 23.6$ MHz.²³ Although the result obtained in the light of Eq. (3) ($\nu_Q \approx 100$ KHz and $\eta \approx 0.98$) should be taken with some caution, the discrepancy with the estimates in Eq. (5), especially for the asymmetry parameter, can be taken as an indication that Li⁺ occupies a position somewhat displaced from the Cu site in the unit cell

Another indication on the location of the Li⁺ could come from the field at the nucleus in the AF phase. We carried out a standard lattice sum $\mathbf{h}_{\text{Li}} = \sum_j \mathcal{D}_j \mathbf{S}_j$, \mathcal{D}_j being the dipolar coupling tensor of the Cu spin \mathbf{S}_j , in the assumption that $\mu_{\text{Cu}} = 0.65\mu_B$ and for the 3D ordered magnetic structure indicated by neutron scattering.³ Several positions in the unit cell were scanned and at least two sites [Cu lattice site and $(0, \frac{1}{2}, 0)$ site] yielded values of $|\mathbf{h}_{\text{Li}}|$ close to the experimental one. The $(0, \frac{1}{2}, 0)$ site can be ruled out, since in this case the EFG would be an order of magnitude larger than the experimental one. Therefore, only a conclusion of qualitative value can be extracted from Li NMR spectra: Li enters in a position somewhat displaced from the Cu lattice site, replacing the Cu²⁺ ion. A search of the Li position by means of neutron scattering did not yield conclusive results in view of the small content of Li.²² It should be remarked that the exact location of the Li ion is not of direct relevance for the interpretation of the relaxation rates in terms of Cu²⁺ low-energy spin excitations (see later on).

For the magnetic field at the Cu nucleus one can refer to a hyperfine Hamiltonian of the form

$$\mathcal{H} = \mathbf{L} \mathbf{A} \mathbf{S} + \mathbf{I} \sum_i \mathcal{B}_i \mathbf{S}_i, \quad (6)$$

with an on-site coupling tensor \mathcal{A} and an isotropic transferred hyperfine interaction with the 12 adjacent Cu²⁺ spins \mathbf{S}_i . The interspin dipolar contribution should be negligible. From symmetry arguments the transferred hyperfine tensors can be grouped in only four independent \mathcal{B}_i .

The magnetic hyperfine tensor at the Cu nucleus in CuO has been derived from paramagnetic shift measurements in the powder above *T_N*.¹⁷ The principal axis of the shift tensor are close to the ones for the EFG and the components of the hyperfine tensor at the Cu nucleus have been estimated: $\mathcal{S}_z^{\text{Cu}} = -146 \pm 10$ KOe/ μ_B and $\mathcal{S}_x^{\text{Cu}} = \mathcal{S}_y^{\text{Cu}} = 15 \pm 15$ KOe/ μ_B .

In the AF phase the 3D ordered Cu moments are aligned along the [010] direction and tilted by nearly 30° from the *z* axes of the hyperfine coupling tensor. The field at the Cu nucleus is 117 KG, at *T* = 4.2 K. A de-

tailed study of the hyperfine tensor in the AF phase has been carried out recently through AFNMR experiments on CuO single crystals.¹⁵ The hyperfine tensor in the AF phase differs from the one in the *P* phase simply by a scalar factor related to the difference in the orientations of the neighboring magnetic ions, through the second term in Eq. (6).

B. Relaxation rates, spin fluctuations, and effects of Li⁺

1. Paramagnetic phase

The relaxation transition probability W associated with the time-dependent part of the magnetic nucleus-electron Hamiltonian can be written

$$W = \frac{\gamma^2}{4} \int \langle h_+(0)h_-(t) \rangle e^{-i\omega_R t} dt, \quad (7)$$

where h_{\pm} are the transverse components of the effective magnetic field at the nucleus with respect to the quantization axis. For ⁷Li NMR relaxation the quantization axis is given by the external magnetic field. For ⁶³Cu NQR relaxation above T_N the quantization axis is the *z* axis of the EFG, while below T_N the combination of the EFG and of the internal magnetic field should be considered.

Let us first discuss the ⁶³Cu and ⁷Li relaxation rates for $T \gg T_N$, where one has ${}^{63}W = 600 \text{ s}^{-1}$ and ${}^7W = 2 \text{ s}^{-1}$ (see Figs. 5 and 6 and Refs. 12 and 13 for pure CuO). In the infinite temperature limit the Cu²⁺ spins are uncorrelated and from Eq. (7), by considering that ω_R is much smaller than the characteristic fluctuation frequency Γ_0 , one can write

$$W(\infty) = \frac{1}{4} \gamma^2 h_{\perp}^2 \frac{1}{\Gamma_0}. \quad (8)$$

By using for the effective field $(h_{\perp}^{\text{Cu}})^2 = [(h_x^{\text{Cu}})^2 + (h_y^{\text{Cu}})^2] \simeq 220 \cdot 10^6 \text{ G}$,^{2,17} the experimental value for ⁶³Cu is given by Eq. (8) in correspondence to $\Gamma_0 = 4 \cdot 10^{12} \text{ rad/s}$. This frequency is smaller than the exchange frequency

$$\omega_e = [8nS(S+1)]^{1/2} J / \hbar \simeq 10^{14} \text{ rad/s},$$

when evaluated for a superexchange constant $J = 460 \text{ K}$ (Ref. 9) and for a number of nearest-neighbor magnetic ions $n = 2$. One should first note the large uncertainty in the transverse components of the effective field ($15 \pm 15 \text{ KOe}/\mu_B$). However, if Eq. (8) is used for ⁷Li W by taking for h_{\perp} the value estimated from a lattice dipolar sum one obtains $\Gamma_0 = 2.5 \times 10^{12} \text{ rad/s}$, in substantial agreement with the estimate from ${}^{63}W(\infty)$ and still yielding a value for Γ_0 much smaller than ω_e .

A possible explanation of this discrepancy is that at $T \simeq 350 \text{ K}$ the Cu²⁺ spins are already strongly correlated. For correlated spin dynamics the field components in Eq. (7) have to be related to the collective spin operators $S_q(t)$. This brings in the correlation function for the normal excitation at wave vector q , thus expressing W in terms of the generalized susceptibility $\chi^{\alpha\alpha}(q, \omega_R)$ or equivalently in terms of the static structure factor $|S_q|^2$ and of the collective spin-fluctuation frequency Γ_q .^{24,25} For $\Gamma_q \gg \omega_R$ in the assumption of spin isotropy, one has

$$\begin{aligned} W &= \frac{\gamma^2}{(2\pi)^2} KT \sum_q (h_q^{\perp})^2 \chi_{\perp}(q, 0) J_q^{\perp}(\omega_R) \\ &= \frac{\gamma^2}{4N} \sum_q (h_q^{\perp})^2 \frac{|S_q|^2}{\Gamma_q}, \end{aligned} \quad (9)$$

where $(h_q^{\perp})^{\text{Cu}} = \mathcal{A}_{\perp} + \sum_i e^{iqr} \mathcal{B}_i$ for ⁶³Cu, while for ⁷Li $(h_q^{\perp})^{\text{Li}} = \sum_i e^{iqr} \mathcal{D}_i$, \mathcal{D}_i being the dipolar coupling tensor.²⁴

By resorting to conventional scaling arguments for the q dependence,^{24,25} Eq. (9) becomes

$$W = \frac{\gamma^2}{2} h_{\text{eff}}^2 \frac{1}{\Gamma_0 \xi^{-z+d-2}}, \quad (10)$$

where for Cu h_{eff} is given by the transverse component of the field at the nucleus measured in the ordered phase,^{14,15} while for Li, in view of the dipolar Hamiltonian (which involves also the longitudinal fluctuations), h_{eff} should be close to the total amplitude of the dipolar field. In Eq. (10) ξ is the magnetic correlation length (in lattice units) and z the dynamical critical exponent; d is the lattice dimensionality, while $\Gamma_0 \xi^{-z}$ has the meaning of a damping constant for overdamped paramagnons.

By comparing Eq. (8) with Eq. (10) one sees that Γ_0 is decreased by a factor around ξ^{-z-2+d} , which can be sizeable in CuO, where at 234 K one has²⁶ $\xi \simeq 150 \text{ \AA}$ along the $[10\bar{1}]$ direction and $\xi \simeq 30 \text{ \AA}$ along the $[101]$ direction.

In the temperature range from 270 up to 500 K (data not reported in Fig. 5) the Cu W is almost constant. A temperature independence of the relaxation rate can hardly be fitted by Eq. (10) by using for $\xi(T)$ the form suggested by $S = \frac{1}{2}$ models for Heisenberg systems at restricted dimensionality.^{27,28} This is surprising, since in 1D and 2D Heisenberg AF's a satisfactory agreement with the predictions from theoretical models is usually found.^{25,29} One could argue that another mechanism, rather than thermal fluctuations, drives the Cu²⁺ spin dynamics in the high-temperature range. A possible candidate is the mechanism of valence fluctuations between Cu²⁺ $3d^9$ and Cu⁺ $3d^{10}$ states, with the hole being transferred to the oxygen.²¹ Then Eq. (8) should basically hold and Γ_0 would correspond to the frequency of valence fluctuations. One should remark that an effective frequency $\Gamma_0 \simeq 3.2 \times 10^{12} \text{ rad/s}$ is also indicated by inelastic neutron scattering.¹

On approaching T_N^+ the relaxation rates show a marked increase (see Figs. 5 and 6), with a relaxation mechanism that appears unrelated to the extent of doping (Fig. 8). The maximum in W marks the transition to the ordered state, provided that the spin-fluctuation frequencies Γ_q remain larger than ω_R , as it is usually the case.²⁴ The *P*-AF transition should be related either to the coupling between Cu-O-Cu chains or to anisotropy factors breaking the rotational invariance of the Heisenberg spins, noticeably the *XY* exchange anisotropy.³⁰ The crossover to an *XY*-like system can be expected to occur when the reduced anisotropy $(g\mu_B H_A / nJS) \xi_{\text{cross}}^2$ is around 1. For $n = 2$ and if one uses for the anisotropy field H_A the value $H_A = 900 \text{ G}$,⁹ this condition implies

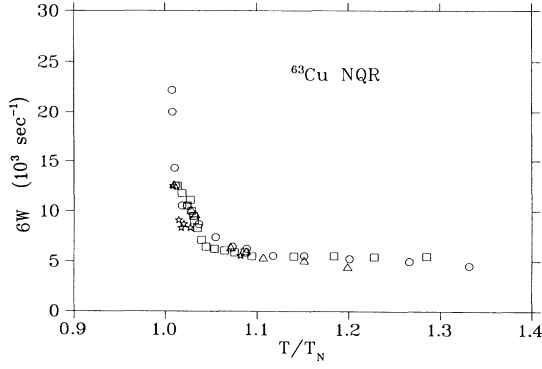


FIG. 8. ⁶³Cu NQR relaxation rates in Cu_{1-x}Li_xO vs the normalized temperature T/T_N . The symbols are the same as in Fig. 5.

$\xi_{\text{cross}} \approx 57$ lattice units, which is not far from the experimental value for ξ along the $[10\bar{1}]$ direction.²⁶ One should remark that also the dipolar field at the Cu nucleus (≈ 500 G) is sizeable enough to drive a crossover towards an Ising-like behavior. In favor of a crossover towards an XY system there is the analogy with the relaxation rates measured for $T \approx T_N^+$ in VCl₂.³¹ A sudden increase in W is observed, while the P -AF transition in this system is believed to involve a Kosterlitz-Thouless mechanism.

In the transition region the relaxation rate expected on the basis of Eq. (10) should behave as $W \propto (T - T_N)^{-n}$, with a critical exponent n depending on the dimensionality, the exponent z and the critical temperature dependence of ξ .^{24,25} For the sake of illustration in Fig. 9, the temperature behavior of the ⁶³Cu NQR relaxation rates is compared to a critical one, by assuming for T_N the values derived from ⁷Li measurements (Table I). A critical exponent $n \approx 0.5$ does not appear unrealistic, although the uncertainties in T_N and the narrow temperature range make this kind of analysis rather uncertain.

Finally, a brief mention about the rapid divergence of the ⁶³Cu spin-spin dephasing time T_2 for $T \rightarrow T_N^+$ is in order. It has been pointed out, in high- T_c superconductors, that an extra contribution to the Cu nuclear spin-spin

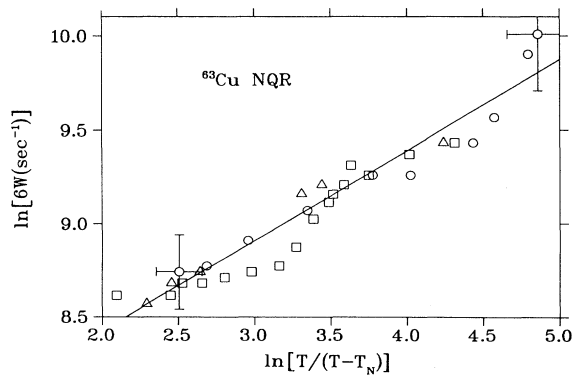


FIG. 9. ⁶³Cu NQR relaxation rates for $T \rightarrow T_N^+$ as a function of $\ln[T/(T - T_N)]$. The solid line corresponds to a critical exponent $n = \frac{1}{2}$. The symbols are the same as in Fig. 5.

coupling arises because of the polarization related to the electron-nucleus hyperfine interaction.³² This contribution involves the coupling of nuclei within a distance of the order of ξ and can be related to the real part of the generalized susceptibility. Since the hyperfine Hamiltonian for the planar Cu in the high- T_c superconductors is similar to Eq. (6) one can expect that a similar contribution to the transverse relaxation rate can exist in CuO. In this case, besides the transverse relaxation rate analogous to W ,²⁴ one has to include a nuclear spin-spin coupling that, to a good approximation yields a term proportional to the magnetic correlation length.³²

2. Antiferromagnetic phase

First we will briefly discuss the case of pure CuO. Then the effect of the Li⁺ ions in the AF phases will be addressed by considering in detail the behavior of the ⁶³Cu and ⁷Li relaxation rates in Cu_{1-x}Li_xO.

In the low-temperature range ($T \ll T_N$) CuO is a 3D antiferromagnet with anisotropy in the static susceptibility and in the magnon spin waves.^{1,33} To discuss the nuclear relaxation one has to take into account the presence of a gap in the spin-wave spectrum, given by $\Delta = g\mu_B \sqrt{2H_A H_{\text{exch}}}/\hbar$. Since $\Delta \gg \omega_R$, the gap prevents the relaxation driven by a direct process, in which a nuclear spin flip is accompanied by emission or absorption of a quantum lattice excitation of energy $\hbar\omega_R$. The effective relaxation mechanism is the Raman two-magnon process.^{34,35} In order to derive a relaxation rate to be used for order of magnitude comparisons in CuO in the limit $T \rightarrow 0$, we will refer to the 3D isotropic AF with a single superexchange interaction, by using for the effective field of the hyperfine interaction the transverse component $|h_{\perp}| \approx 49$ KG, with a quantization axis forming an angle $\alpha \approx 30^\circ$ with the direction of the \mathbf{S} spin alignment (see Sec. III A). Then, for the two-magnon process, one has

$$W = \gamma^2 h_{\perp}^2 \frac{4 \sin^2 \alpha}{(2\pi)^3 \omega_e} \left[\frac{KT}{\hbar\omega_e} \right]^3 \int_{\hbar\Delta/KT}^{\infty} \frac{x dx}{e^x - 1}, \quad (11)$$

with $x = \hbar\omega_q/KT$ and $\omega_q = (\Delta^2 + c^2 q^2)^{1/2}$. In CuO, Δ can be estimated around 14 K (see Sec. III B). Thus for $T \geq 20$ K one can write Eq. (11) in the approximate form

$$W \approx \gamma^2 h_{\perp}^2 \frac{2.35\pi^2}{(2\pi)^3 6\omega_e} \left[\frac{T}{T_{\text{exch}}} \right]^3, \quad (12a)$$

while for $T \ll \Delta$ one has

$$W \approx \gamma^2 h_{\perp}^2 \frac{2.35}{(2\pi)^3 \omega_e} \left[\frac{T}{T_{\text{exch}}} \right]^3 \left[\frac{\hbar\Delta}{KT} \right] e^{-\hbar\Delta/KT}. \quad (12b)$$

The temperature dependence of our data for ⁶³Cu W in CuO for $T \leq 77$ K, which are in good agreement with recent measurements by Tsuda, Ohno, and Yasuoka,³⁶ is satisfactorily described by Eqs. (12). As regards the absolute value, Eq. (12a), by using $\omega_e = 10^{14}$ rad/s (see Sec. III B 1) and $T_{\text{exch}} = 460$ K, yields $W \approx 8 \times 10^{-3} \text{ s}^{-1}$, at $T = 77$ K. The large discrepancy with the experimental result, $W = 6 \times 10^{-1} \text{ s}^{-1}$ (Fig. 7), can be due to a break-

down of the small q approximation and/or to the anisotropy in the spin excitations, as already noticed.³⁶ However, an approximate estimate of W by taking into account two different superexchange constants (namely one along the $[10\bar{1}]$ direction and one along the $[101]$ direction) gives a relaxation rate of the same order of magnitude of the one estimated from Eq. (12a). At $T=4.2$ K one measures $W=2.4\times 10^{-3}$ s⁻¹ (see Fig. 7) and Eq. (12b) yields $W\simeq 10^{-3}$ s⁻¹, indicating that for $T\rightarrow 0$ the theoretical predictions fit better the experimental result. In the light of the subsequent discussion on the effects of charge defects on the spin dynamics, one should also take into consideration the possibility of nonperfect oxygen stoichiometry in nominally pure CuO, causing an extra contribution to the relaxation in the temperature range 15–100 K (see later on).

The drastic decrease of the ⁶³Cu relaxation rates at low temperatures with respect to the ones in the PA phase can be interpreted in terms of an effective spectral density $J_{\text{eff}}(\omega\rightarrow 0)=1/N\sum_q J(\mathbf{q},\omega\rightarrow 0)$ becoming negligible in the rf range when the excitations are AF spin waves in the presence of a gap. A striking experimental finding is that the W 's in the AF phase increase by orders of magnitude upon Li doping, corresponding to a marked increase of J_{eff} (see Fig. 7). An analogous effect has been noticed in comparing the ⁶³Cu W in CuO with the ones in YBa₂Cu₃O₆ and La₂CuO₄.³⁶

To discuss the spin dynamics in the AF phase of Cu_{1-x}Li_xO let us first recall that at finite temperature ($T\leq T_N$) the excitations in 2D $S=\frac{1}{2}$ AF's exhibit relevant modifications with respect to the conventional spin-wave spectrum of a 3D ordered AF. In fact, low-energy (<15 meV) neutron scattering in La₂CuO₄ shows that the spin fluctuations for $q\simeq q_{\text{AF}}$ are characterized by a relaxational correlation function, with a quasielastic peak of width $\hbar\Gamma$ around 4 meV in the q -integrated spectral density.³⁷ For $T\simeq T_N$ propagating spin waves can exist only in short-range ordered regions of size ξ , namely for wave vectors larger than ξ^{-1} . The experimental findings correspond to regions of magnetization density short-range ordered in space which relax with a time scale related to ξ^{-1} .

The possible occurrence of a central component in the spectral density having this origin should be considered in the AF phase of Cu_{1-x}Li_xO, since the presence of charge and spin Li⁺ defects can cause "boundary" disordering effects overdamping the spin waves or, equivalently, inducing a relaxational dynamics of short-range ordered AF "islands" of correlated Cu²⁺ spins. To discuss these effects it is convenient to model the collective spectral density $J(q,\omega)$ in the form

$$J(q,\omega)=\frac{1}{2\pi}\left[\frac{\Gamma_{\text{SF}}}{(\omega-\omega_q)^2+\Gamma_{\text{SF}}^2}+\frac{\Gamma_{\text{SF}}}{(\omega+\omega_q)^2+\Gamma_{\text{SF}}^2}\right] \quad (13)$$

where Γ_{SF} heuristically describes the relaxational dynamics, while $\omega_q=(\Delta^2+c^2q^2)^{1/2}$. Although Eq. (13) might be an oversimplification, it has been conveniently used in the interpretation of neutron scattering in disordered 2D AF's.^{38,39}

From Eq. (13), by integrating over q for $\omega\rightarrow 0$ one

derives

$$J_{\text{eff}}=\frac{1}{2}\frac{1}{\Gamma_{\text{SF}}}\left[\frac{\Gamma_{\text{SF}}}{\Gamma_{\text{SW}}}\right]^2\ln\frac{\Gamma_{\text{SW}}^2+\Delta^2+\Gamma_{\text{SF}}^2}{\Delta^2+\Gamma_{\text{SF}}^2} \quad (14)$$

having indicated with $\Gamma_{\text{SW}}=cq_m$ ($q_m\simeq\pi/a$, maximum wave vector) a typical spin-wave frequency. For an order of magnitude estimate one can use $\hbar\Gamma_{\text{SW}}=\hbar cq_m\simeq 65$ meV for the magnon dispersion curve along the $(0,q,0)$ in CuO.³³ Γ_{SF} is hardly derived by neutron scattering because of resolution limits. A value in the meV range is indicated¹ and it is reasonable, also in view of the similarities with La₂CuO₄.³⁷ Then, from Eq. (14) one obtains $J_{\text{eff}}\simeq 2\times 10^{-16}$ rad/s, a factor of 50 larger than $J_{\text{eff}}=(6\times 10^{-2}/\omega_e)(T/T_{\text{exch}})^3$ expected from Eq. (12a), at $T=77$ K, and leading to a value of W in satisfactory agreement with the experimental data in CuO. It can also be noted that for overdamped, nonpropagating paramagnons Γ_{SW} must be taken of the order of Γ_{SF} and Eq. (14) gives the form of the relaxation rates used in the P phase, with a q -integrated frequency becoming the equivalent of Γ_{SF} [see Sec. III B].

Thus it seems possible to conclude that even in nominally pure CuO, at least for $T\geq 77$ K, a sizeable contribution to the ⁶³Cu relaxation comes from the direct process through a central component in the spectrum of the excitations. Now we are going to discuss in more details the x and T dependence of this central component in Cu_{1-x}Li_xO.

From Fig. 7 one sees that upon Li doping the effective spectral density grows approximately as $J_{\text{eff}}\propto\exp(x/x^*)$, with $x^*\simeq 6\times 10^{-3}$, at $T=77$ K. Such a dramatic insurgence cannot be justified in terms of usual impurity effects in conventional AF systems where much larger amounts of impurities are necessary to induce appreciable modifications and the effect on the spectral density is moderate and spatially limited.⁴⁰ As regards the temperature dependence, while in pure CuO one has a continuous decrease of W on decreasing temperature, in Cu_{1-x}Li_xO a marked increase of ⁶³W is present below $T\simeq 80$ K. The spin-spin relaxation time becomes so short that the ⁶³Cu signal is lost in a temperature range from about 15–50 K (data not reported in the figures). An enhancement of the relaxation rate analogous to the one reported here for Cu_{1-x}Li_xO has been noted in comparing the ⁶³Cu W in AF CuO with the ones in the AF phases of La₂CuO₄ and YBa₂Cu₃O₆,³⁶ as already mentioned. A large low-energy spectrum of spin excitations has been inferred also in YBa₂Cu₃O_{6.1} from the temperature dependence of the Cu(2) AFNMR frequency.⁴¹

One could attempt an interpretation of the temperature behavior of W 's in Cu_{1-x}Li_xO on the basis of the expected slowing down of $\Gamma_{\text{SF}}(x,T)$ for $T\rightarrow 0$, a maximum in W occurring when Γ_{SF} reaches the radio frequency range. An inspection to Eq. (14) rules out this possibility, since a decrease of Γ_{SF} reduces J_{eff} . In the light of the arguments underlying Eq. (14), the decrease of J_{eff} is the consequence of the decreasing number of modes contributing to the central component when Γ_{SF} is reduced. To explain the presence of a sizeable amount of spin excitations in the MHz range one has to look for an extra

mechanism leading to a quasielastic central peak in the spectral density. The difference between the quasielastic peak and the contribution from spin waves at finite q and ω has been discussed in the interpretation of the neutron-scattering cross section of the “disordered” 2D AF La₂CuO₄ for T close to T_N .³⁷

3. Low-energy spin excitations from mobile holes

A strong central component in J_{eff} can reflect the resurgence of low-energy spin excitations when mobile holes are induced in an AF matrix. In particular, it has been shown⁴² in the framework of the t - J model that a mobile spin vacancy in an AF matrix (as the one resulting from the Zhang-Rice singlet in the AF precursors of high- T_c superconductors) can allow a spin flip at zero energy cost when a simultaneous hopping of the vacancy itself occurs. On the other hand it has been proven⁴³ by means of K -edge x-ray-absorption spectroscopy that in Ni_{1-x}Li_xO, and most likely in Cu_{1-x}Li_xO also, the holes compensating the lithium charge are located primarily in O_{2p} states, as occurs for instance in Sr-doped La₂CuO₄. Mobile defects, namely extended but localized regions of “disturbed” spins, are well known in low dimensional magnetic systems, where they have been considered as solitons, skyrmions, magnetic polarons, etc. For instance, the critical broadening of electron paramagnetic resonance (EPR) line in 2D AF's could be explained by mobile 2D solitons.⁴⁴ The temperature behavior of ¹³⁹La NQR relaxation rates in La_{2-x}Sr_xCuO₄ has been justified through a picture of mobile charge defects locally disturbing a given spin configuration.^{45,46} The correlation length is expected to be limited by the concentration x , namely $\xi \approx 1/x^{1/D}$, and a relationship of the form $\xi \approx 1/\sqrt{x}$ has been found in 2D La_{2-x}Sr_xCuO₄ by neutron scattering.^{47,48}

In order to describe the contribution to the spectral density J_{eff} from the holes induced in the Cu-O band by the heterovalent substitution, in the AF phase, it is convenient to refer first to the ⁷Li NMR relaxation. In this case, in fact, the strong external field represents the fixed

quantization axis and defines the Zeeman eigenstates, while the fluctuations in the local Cu²⁺ spin configuration act on Li nuclei through the relatively small dipolar interaction. Therefore the ordinary weak-collisions approach and time-dependent perturbation theory can be used. A simple description can be given by considering the dipolar magnetic field $\mathbf{h}_i(t, \mathbf{r})$ at the Li site due to the i th hole. On the basis of the similarity with the relaxation due to diffusing charges⁴⁹ we assume an exponential isotropic correlation function, with a characteristic correlation time $\tau(r)$ given by $\tau(r) = (r/b)^2 \tau_h$, where b is an average lattice step and τ_h is the average “diffusion” time of the hole. τ_h describes the loss of correlation of the local AF configuration and it is related to the fraction of mobile defects $n_h(x, T)$. τ_h can be interpreted as the mean time interval between consecutive passages of the hole at a given site. Then $\tau_h \approx \tau_0/n_h$, τ_0^{-1} being of the order of the exchange frequency, consistently with the t - J model. In a similar picture⁵⁰ the time for the annealing of a local spin configuration has been written $\tau_h \approx 1/\Delta_h n_h$, Δ_h being the bandwidth.

By using for \mathbf{h} the magnetic field describing the dipolar interaction and considering also the time dependence due to the precessional frequencies of the electronic spins,^{24,25} one can write Eq. (7) in the form

$$W = \frac{\gamma^2}{8} \hbar^2 \gamma_e^2 9 \int_V \left[\alpha_1 J_{\parallel}(\omega_L) + \frac{\alpha_2}{4} J_{\perp}(\omega_e) + \frac{\alpha_0}{36} J_{\perp}(\omega_e) \right] c_h r^2 dr d\Omega, \quad (15)$$

with $\alpha_0 = (1 - 3 \cos^2 \theta)^2 / r^6$, $\alpha_1 = \sin^2 \theta \cos^2 \theta / r^6$, and $\alpha_2 = \sin^4 \theta / r^6$, c_h being the hole concentration. The damping in the precessional motions of the electron spin due to the disorder allows one to shift the spectral densities \mathcal{J} 's for the field \mathbf{h} in Eq. (15) to ω_L . By taking into account that $\bar{\alpha}_0 = \frac{8}{10} r^{-6}$, $\bar{\alpha}_1 = \frac{2}{15} r^{-6}$, and $\bar{\alpha}_2 = \frac{8}{15} r^{-6}$ one obtains

$$\begin{aligned} W &= \frac{\gamma^2}{8} \mu_{\text{Cu}}^2 \frac{109}{90} \int_{d_m}^{\infty} \frac{c_h}{r^6} \frac{2\tau(r)}{1 + \omega_L^2 \tau^2(r)} r^2 dr \\ &= 3/10 \gamma^2 (a \mu_{\text{Cu}})^2 \frac{c_h}{b^2 d_m} \tau_h \left\{ 1 + \frac{d_m \sqrt{2\omega_L \tau_h}}{8b} \left[\ln \frac{d_m^2 - 2kd_m + 2k^2}{d_m^2 + 2kd_m + 2k^2} + 2 \tan^{-1} \left[\frac{2kd_m}{2k^2 - d_m^2} \right] \right] \right\} \\ &\approx 3/10 \gamma^2 (a \mu_{\text{Cu}})^2 \frac{c_h}{b^3} \tau_h \left\{ 1 + \frac{\sqrt{2\omega_L \tau_h}}{4\sqrt{2}} \left[\ln \frac{\omega_L \tau_h - \sqrt{2\omega_L \tau_h} + 1}{\omega_L \tau_h + \sqrt{2\omega_L \tau_h} + 1} + 2 \tan^{-1} \left[\frac{\sqrt{2\omega_L \tau_h}}{1 - \omega_L \tau_h} \right] \right] \right\}, \quad (16) \end{aligned}$$

where $k = b/\sqrt{2\omega_L \tau_h}$, while in the last term of the equation the minimum distance of approach of the hole to the Li ion d_m has been assumed equal to the average lattice step b . In Eq. (16), a is a constant of the order of some units which accounts for the extended character of the

magnetic polaron induced by the hole.

According to Eq. (16), a maximum in the relaxation rate occurs for $\tau_h \approx \omega_L^{-1}$. Utilizing this condition we can test the validity of our picture by comparing the theoretical estimate of \mathcal{W}_{max} at $T = T_{\text{max}}$ with the experimental

data. By using in Eq. (16), $\mu_{\text{Cu}} = 0.69\mu_B$, $b = 3 \text{ \AA}$, and for the hole concentration $c_h = 1.5 \times 10^{21} \text{ cm}^{-3}$ (correspondent to $x = 0.03$) for $\text{Cu}_{0.97}\text{Li}_{0.03}\text{O}$, one obtains $2W_{\text{max}} = 3.2a^2 \text{ s}^{-1}$, consistent with the experimental data for $a \approx 2-3$ (see Fig. 6). This order of magnitude agreement is a strong support to the hypothesis of the Cu^{2+} spin fluctuations controlled by the diffusion of holes in the CuO band. Another confirmation comes from the frequency dependence of the relaxation rates (see later on).

Let us first consider Eq. (16) in the temperature range where the condition of fast modulations can be used, namely $\tau_h \ll \omega_L^{-1}$, ω_L being the Larmor angular frequency for ${}^7\text{Li}$ in the external field. In practice this condition corresponds to $T \geq T_{\text{max}} = 70 \text{ K}$ for $x = 0.02$ and to $T \geq T_{\text{max}} = 35 \text{ K}$ for $x = 0.03$ (see Fig. 6). Then Eq. (17) becomes

$$W \approx \frac{3}{10} \gamma^2 a^2 \mu_{\text{Cu}}^2 \frac{\tau_h c_h}{b^2 d_m}, \quad (17)$$

and insights on the x and T dependence of τ_h can be obtained from the experimental results for W . By indicating with $E = E(x)$ the energy gap from localized to itinerant states, the fraction of delocalized mobile holes can be written $n_h(x, T) = n_h(x, \infty) e^{-E(x)/T}$. Then one has

$$\tau_h \approx \frac{\tau_0}{n_h} \approx \frac{\tau_0}{x} e^{E(x)/T}. \quad (18)$$

An effective correlation time τ_h of the form given in Eq. (18) was found^{45,46} to justify the divergence, on cooling, of the ${}^{139}\text{La}$ NQR relaxation rates in $\text{La}_{2-x}\text{Sr}_x\text{CuO}_4$, for $0.02 \leq x \leq 0.05$ and for T not too close to T_N . (On approaching the transition to the ordered state a change-over in the T dependence of W has been more recently detected;⁵¹ furthermore, for $x \leq 0.02$ the phase diagram in $\text{La}_{2-x}\text{Sr}_x\text{CuO}_4$ shows first the P -AF transition followed by a reentrant transition to a spin-glass phase, depending also from the oxygen stoichiometry.⁵²)

One would expect that the mobile holes play some role in the electrical conductivity, at least for certain ranges of x and T . We are aware of only few resistivity measurements in $\text{Cu}_{1-x}\text{Li}_x\text{O}$.⁵³ A drastic increase of the conductivity actually occurs upon Li doping and an effective activation energy is x dependent, as one would qualitatively expect in the light of the aforementioned arguments.

In Fig. 10 the ${}^7\text{Li}$ relaxation rates are analyzed in the light of the behavior theoretically expected from Eqs. (17) and (18) in the condition of fast fluctuations, for $T \geq T_{\text{max}}$. The experimental results are rather well fitted, yielding $E(x = 0.03) \approx 200 \text{ K}$ and $E(x = 0.02) \approx 310 \text{ K}$. These values support the hypothesis of a gap between localized and itinerant states strongly decreased by charge doping, similarly to the case of lanthanum oxides.

Finally, a comment on the results for W below T_{max} is in order. For $T \leq 70 \text{ K}$ in the 2%-doped sample and for $T \leq 34 \text{ K}$ in the 3% sample the diffusion of the holes is

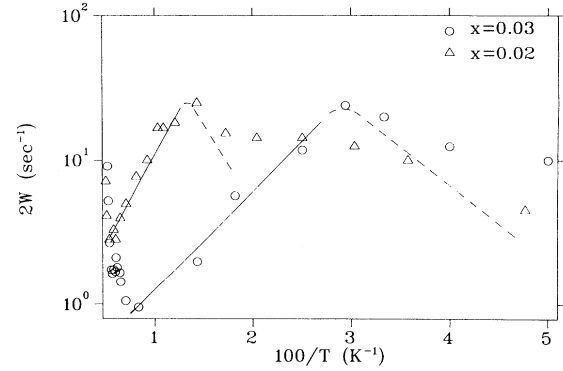


FIG. 10. Comparison of the ${}^7\text{Li}$ NMR relaxation rates in the AF phase of $\text{Cu}_{1-x}\text{Li}_x\text{O}$ (see Fig. 6) with the theoretical behaviors. The solid lines are the best fits for fast fluctuations and yield $E(x)$. The dotted lines represent W in the slow fluctuations regime ($\omega_L \tau_h \gg 1$) for a monodispersive diffusionlike process.

characterized by τ_h longer than ω_L^{-1} (slow fluctuations regime). In the hypothesis of a single effective correlation time, from Eq. (16) in the limit $(\tau_h \omega_L)^2 \gg 1$ one would expect $W \propto \omega_L^{-2} \tau_h^{-1}$ (see the dotted lines in Fig. 10). A departure of the experimental data from the behavior correspondent to a monodispersive diffusionlike process seems to occur in the lowest temperature range. In disordered systems a distribution of correlation times and correlation functions of the stretched exponential type are common aspects. For moderate disorder, i.e., x small, the behavior of the relaxation rates takes a form similar to the one in Fig. 10, with an apparent monodispersive side for $T > T_{\text{max}}$ and a departure below.⁵⁴

A decisive test for the validity of our picture is the frequency dependence of ${}^7\text{Li}$ W . In spite of the reduced sensitivity, reliable measurements of ${}^7\text{Li}$ W could be carried out in $\text{Cu}_{0.97}\text{Li}_{0.03}\text{O}$ in a field reduced to $H_0 = 17 \text{ K G}$, corresponding to $\nu_L = 28 \text{ MHz}$. As shown in Fig. 11, for this frequency the maximum in W is shifted some degrees below the one for $\nu_L = 97.5 \text{ MHz}$. Furthermore $W_{\text{max}}(\nu_L = 28 \text{ MHz})$ is greater than $W_{\text{max}}(\nu_L = 97.5 \text{ MHz})$ by a factor ≈ 3.46 very close to the value 3.48 expected in the light of Eq. (16).

As regards the Cu relaxation in the AF phase of $\text{Cu}_{1-x}\text{Li}_x\text{O}$, the relevant difference with respect to the case of ${}^7\text{Li}$ is that for the Cu nucleus the passage of the spin polaron alters the local quantization axes. This corresponds to a "strong-collisions" effect, in which one has a sudden motion of the Zeeman eigenstates.⁵⁵ A theoretical description of the relaxation process driven by this mechanism is difficult and beyond the purpose of this paper. Qualitatively one can say that in the fast motions regimes, namely $\tau_h^{-1} \gg \omega_{\text{AFNMR}}$, the occurrence of many events during a Larmor period should still allow one to apply a time-dependent perturbation approach and equations similar to the ones for ${}^7\text{Li}$ relaxation should be applicable. Since the strength of the perturbation is much larger than the one for Li, the correspondent relaxation process for Cu is much more effective (by a factor of the

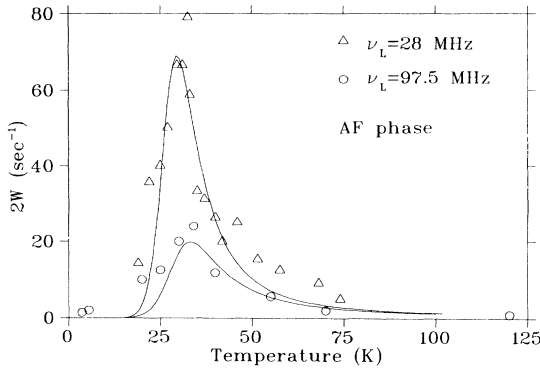


FIG. 11. Comparison of ⁷Li relaxation rates in Cu_{0.97}Li_{0.03}O for two measuring frequencies ν_L . The solid lines correspond to the theoretical forms according to Eqs. (16) and (18) of the text, for $E(0.03)=200$ K as obtained from the slope of W vs $100/T$ (see Fig. 10) in the fast fluctuations regime.

order of the square of the ratio of effective fields, namely about 10^4). This description breaks down when the condition of slow motions is progressively approached. For $\tau_h^{-1} \leq \omega_{\text{AFNMR}}$, by applying general arguments⁵⁵ one could say that the relaxation time is of the order of the correlation time itself, $W \simeq \tau_h^{-1}$. The lack of the Cu AFNMR signal in Cu_{1-x}Li_xO in the temperature range 15–55 K is consistent with the above considerations. At lower temperatures the ⁶³Cu AFNMR signal is again detectable, since τ becomes longer, corresponding to the progressive localization of the holes, according to Eq. (18).

IV. SUMMARIZING REMARKS

From a variety of ⁶³Cu and ⁷Li nuclear-magnetic-resonance and relaxation measurements, enlightening insights into the internal magnetic fields and EFG's and into the Cu²⁺ spin dynamics in Cu_{1-x}Li_xO have been obtained, in the paramagnetic and in the antiferromagnetic phases.

From the fields measured at the Cu and at the Li nuclei it was found that Li⁺ can enter in CuO to an extent of about 4%, while for larger amounts phase segregation occurs. The comparison of the values of the fields and of the EFG's with the ones estimated from lattice sums supports the hypothesis that Li replaces a Cu²⁺ ion, taking a position close to the one of Cu²⁺ itself.

The substitution of Li⁺ for Cu²⁺ increases the nuclear quadrupole coupling constant ν_Q of ⁶³Cu, either because of the charge unbalancement or of the change in the occupation of the 3d orbitals. On approaching T_N in the paramagnetic phase, a dip in ν_Q is detected, somewhat indicative of fluctuations in the electronic configurations.

The Néel temperature is changed by Li doping to a moderate extent, being reduced from $T_N=226 \pm 1$ K in pure CuO to $T_N=183 \pm 1$ K in Cu_{0.963}Li_{0.037}O.

The ⁷Li and ⁶³Cu relaxation rates are driven by the time dependence of the magnetic hyperfine Hamiltonians and allowed us to extract information on the Cu²⁺ spin dynamics. In the paramagnetic phase of Cu_{1-x}Li_xO the

Cu²⁺ spin fluctuations are almost unaffected by Li doping: The relaxation rates W in the P phases are practically x independent and reflect the strong correlation of the Cu²⁺ ions. For $T \gg T_N$ the results for W suggest that the spin dynamics is possibly related to the valence fluctuations, as suggested by x-ray photoelectron spectroscopy. For $T/T_N \simeq 1$, a crossover to an XY-like anisotropic Heisenberg or to an Ising-like behavior in the spin fluctuations appears to drive the transition to the 3D ordered state.

In the AF phase the ordered Cu magnetic moments are aligned parallel to the [010] direction and tilted by nearly 30° from the z axis of the hyperfine coupling tensor, which differs from the one in the P phase only by a scalar factor related to the difference in the orientations of the neighboring magnetic ions.

In pure CuO, in the low-temperature range, the dominant relaxation mechanism is the Raman two-magnon process, corresponding to almost underdamped spin waves in conventional antiferromagnets. The Li doping has been found to alter the Cu²⁺ spin fluctuations in a dramatic way in the AF phase. In fact, the ⁶³Cu W in Cu_{1-x}Li_xO increases by several orders of magnitude with respect to CuO, analogous to the case of copper oxide precursors of high- T_c superconductors. Furthermore, both ⁶³Cu and ⁷Li W 's display temperature behaviors very different from the one in pure CuO, with a marked maximum at a temperature T_{max} , which is a function of x and of the measuring frequency ν_L . These effects can be discussed in terms of a spectral density J_{eff} in the rf range, which is negligible in pure CuO and strongly increased in Cu_{1-x}Li_xO. Two possible sources of this enhancement have been considered, namely boundary disordering effects on the spin waves and the diffusion of local disturbance of the AF matrix (spin-polaron) induced by the heterovalent substitution. The x and T behaviors of W 's rule out a sizeable contribution to $J_{\text{eff}}(\omega \rightarrow 0)$ related to the boundary disordering effects on AF spin waves. On the contrary a satisfactory description of the Cu²⁺ spin dynamics in the AF phase of Cu_{1-x}Li_xO has been obtained by considering the insurgence of low-energy spin excitations related to the diffusion of the holes. A simple picture, based on the idea of a fluctuating dipolar field $\mathbf{h}(\mathbf{r}, t)$ indirectly generated at the Li site by the hole, has been given. In this way J_{eff} has been related to a correlation time of the form $\tau_h \propto (\omega_{\text{exch}} n_h)^{-1} \propto e^{E(x)/T}$, $E(x)$ being the energy gap from localized to itinerant states. The orders of magnitude, x and T dependence of the relaxation rates are satisfactorily explained by this picture. In particular, it has been shown that the correlation time for the hole becomes $\tau_h \simeq 10^{-9}$ s at about $T \simeq 70$ K in Cu_{0.98}Li_{0.02}O and at $T \simeq 34$ K in Cu_{0.97}Li_{0.03}O, and that the energy gap is of the form $E(x) \simeq 6/x$ K. By varying the measuring frequency the ⁷Li relaxation rates are modified in a way quantitatively consistent with the overall picture and with the numerical estimates.

Finally, we remark that because of the frequency range these findings are hard to obtain by other techniques such as neutron scattering and that the results derived in this

work for Li-doped CuO should be of strong interest also in view of the similarities with the AF's precursors of high- T_c superconductors.

ACKNOWLEDGMENTS

Useful discussions with F. Borsa, J. Murgich, F. Parmigiani, and G. Samoggia are gratefully acknowledged. S. Aldrovandi, whose technical assistance was very help-

ful in many respects, is thanked for the specific-heat measurements. Finally we would like to thank A. Lascialfari for his collaboration in carrying out preliminary NQR-NMR measurements in CuO. The research has been performed with the support of INFN (Grant No. MSC-PV), of an INFN-MPI 40% grant, and in the framework of the Progetto Finalizzato "Superconductive and Cryogenic Technologies," sponsored by the National Research Council of Italy, CNR.

- ¹B. X. Yang, T. R. Thurston, J. M. Tranquada, and G. Shirane, *Phys. Rev. B* **39**, 4343 (1989).
- ²S. Asbrink and L. J. Norrby, *Acta Crystallogr. B* **26**, 8 (1970).
- ³J. B. Forsyth, P. J. Brown, and B. M. Wanklyn, *J. Phys. C* **21**, 2917 (1988); see also M. Ain *et al.*, *Physica C* **162-164**, 1279 (1989); and *J. Phys.: Condens. Matter* (to be published); T. Chattopadhyay *et al.*, *Physica C* **170**, 371 (1990).
- ⁴A. Junod *et al.*, *J. Phys. Condens. Matter* **1**, 8021 (1989).
- ⁵M. O'Keeffe and F. S. Stone, *J. Phys. Chem. Solids* **23**, 261 (1962).
- ⁶B. Roden, E. Braun, and A. Freimuth, *Solid State Commun.* **64**, 1051 (1987).
- ⁷S. S. P. Parkin *et al.*, *Phys. Rev. B* **37**, 131 (1988).
- ⁸U. Köbler and T. Chattopadhyay, *Z. Phys. B* **82**, 383 (1981).
- ⁹O. Kondo *et al.*, *J. Phys. Soc. Jpn.* **57**, 3293 (1988).
- ¹⁰J. W. Loram *et al.*, *Europhys. Lett.* **8**, 263 (1989).
- ¹¹T. I. Arbutova *et al.*, *J. Magn. Magn. Mater.* **95**, 168 (1991).
- ¹²J. Ziolo, F. Borsa, M. Corti, and A. Rigamonti, *J. Appl. Phys.* **67**, 5864 (1990).
- ¹³Y. Itoh *et al.*, *J. Phys. Soc. Jpn.* **59**, 1143 (1990).
- ¹⁴T. Tsuda *et al.*, *J. Phys. Soc. Jpn.* **57**, 2908 (1988).
- ¹⁵L. Cristofolini *et al.*, *Physica C* **191**, 97 (1992); L. Cristofolini (private communication).
- ¹⁶L. Martini and F. Parmigiani (private communication).
- ¹⁷T. Shimizu *et al.*, *Bull. Mag. Reson.* **12**, 39 (1990).
- ¹⁸R. G. Graham, P. C. Riedi, and B. M. Wanklyn, *J. Phys.: Condens. Matter* **3**, 135 (1991).
- ¹⁹G. Guidi *et al.*, *Solid State Commun.* **68**, 759 (1988).
- ²⁰A. Rigamonti, *Adv. Phys.* **33**, 115 (1984), and references therein.
- ²¹F. Parmigiani and G. Samoggia, *Europhys. Lett.* **7**, 543 (1988).
- ²²I. Natali Sora (private communication).
- ²³M. E. Garcia and K. H. Bennemann, *Phys. Rev. B* **40**, 8809 (1989).
- ²⁴For details, see F. Borsa and A. Rigamonti, in *Magnetic Resonance at Phase Transitions*, edited by F. J. Owens, C. P. Poole, and H. A. Farach (Academic, New York, 1979), p. 102.
- ²⁵H. Benner and J. P. Boucher, in *Magnetic Properties of Layered Transition Metal Compounds*, edited by L. J. de Jongh (Kluwer, Dordrecht, 1990), p. 323.
- ²⁶T. Chattopadhyay *et al.*, *Physica C* **170**, 371 (1990).
- ²⁷M. Steiner, J. Villain, and C. G. Windsor, *Adv. Phys.* **25**, 87 (1976).
- ²⁸S. Chakravarty, B. I. Halperin, and D. R. Nelson, *Phys. Rev. B* **39**, 2344 (1989).
- ²⁹F. Borsa *et al.*, *Phys. Rev. B* **45**, 5756 (1992).
- ³⁰H.-Q. Ding, *Phys. Rev. Lett.* **68**, 1927 (1992).
- ³¹F. Tabak, A. Lascialfari, and A. Rigamonti, *J. Phys.: Condens. Matter* **5**, 1 (1993).
- ³²C. H. Pennington and C. P. Slichter, *Phys. Rev. Lett.* **66**, 381 (1991).
- ³³M. Ain *et al.*, *Physica C* **162**, 1279 (1989).
- ³⁴T. Moriya, *Prog. Theor. Phys.* **16**, 641 (1956).
- ³⁵D. Beeman and P. Pincus, *Phys. Rev.* **166**, 359 (1968).
- ³⁶T. Tsuda, T. Ohno, and H. Yasuoka, *J. Phys. Soc. Jpn.* **61**, 2109 (1992).
- ³⁷O. Scharpf and H. Capelmann, *Z. Phys. B* **86**, 59 (1992).
- ³⁸See for example, T. Freltoft *et al.*, *Phys. Rev. B* **44**, 5046 (1991) for La_2NiO_4 and S. M. Hayden *et al.*, *Phys. Rev. Lett.* **68**, 1061 (1992) for $\text{La}_{2-x}\text{Sr}_x\text{NiO}_4$.
- ³⁹J. N. Tranquada *et al.*, *Phys. Rev. Lett.* **64**, 800 (1990), and references therein.
- ⁴⁰See, for instance, L. J. de Jongh, in *Magnetic Properties of Layered Transition Metal Compounds* (Ref. 25); p. 1; H. W. De Wijn, *ibid.*, p. 191.
- ⁴¹Y. Iwamoto *et al.*, *J. Phys. Soc. Jpn.* **61**, 441 (1992).
- ⁴²T. Kopp and F. Mila, *Phys. Rev. B* **43**, 12980 (1991).
- ⁴³P. Kuiper *et al.*, *Phys. Rev. Lett.* **62**, 221 (1989).
- ⁴⁴F. Waldner, *J. Magn. Magn. Mater.* **54**, 873 (1986); **31**, 1203 (1983).
- ⁴⁵F. Borsa, M. Corti, T. Rega, and A. Rigamonti, *Nuovo Cimento D* **11**, 1785 (1989).
- ⁴⁶A. Rigamonti *et al.*, in *Early and Recent Aspects of Superconductivity*, edited by J. G. Bednorz and K. A. Muller (Springer-Verlag, Berlin, 1990), p. 441.
- ⁴⁷R. J. Birgeneau *et al.*, *Phys. Rev. B* **38**, 6614 (1988); **39**, 2868 (1989).
- ⁴⁸B. Keimer *et al.*, *Phys. Rev. Lett.* **67**, 1930 (1991).
- ⁴⁹F. Reif, *Phys. Rev.* **100**, 1957 (1955).
- ⁵⁰T. V. Ramakrishnan, *Physica C* **153**, 155 (1988).
- ⁵¹H. Cho *et al.*, *Phys. Rev. B* **46**, 3179 (1992).
- ⁵²F. C. Chou *et al.* (private communication).
- ⁵³R. R. Heikes and W. D. Johnston, *J. Chem. Phys.* **26**, 582 (1957); R. Feduzi, F. Lanza, and V. Dallacasa (unpublished).
- ⁵⁴See some cases illustrated in, F. Borsa and A. Rigamonti, edited by K. A. Muller, J. C. Feyet, F. Borsa, and A. Rigamonti, *Structural Phase Transitions* (Springer-Verlag, Berlin, 1991), Vol. II.
- ⁵⁵D. Wolf, *Spin-Temperature and Nuclear-Spin Relaxation in Matter* (Clarendon, Oxford, 1979), Chap. 9 and 12, and references therein; D. C. Ailon, *Adv. Magn. Res.* **5**, 117 (1972).